Nanoscale

Accepted Manuscript

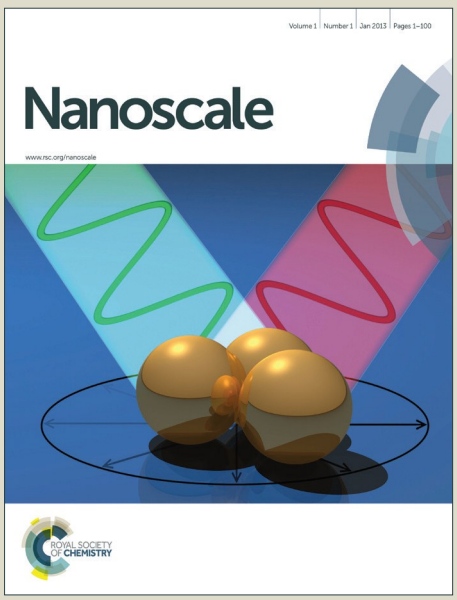

ROYAL SOCIETY OF CHEMISTRY

www.rsc.org/nanoscale

Nanoscale

PAPER

Bifunctional Ultraviolet/Ultrasound Responsive Composite TiO_2/Polyelectrolytes Microcapsules

Received 00th January 20xx,
Accepted 00th January 20xx

DOI: 10.1039/x0xx00000x

www.rsc.org/

Hui Gao,[a] Dongsheng Wen,[b] Nadezda V. Tarakina,[a] Jierong Liang,[a] Andy J. Bushby[a] and Gleb B. Sukhorukov [a*]

Designing and fabricating multifunctional microcapsules are of considerable interest to both academic and industrial research aspects. This work reports an innovative approach to fabricate composite capsules with high UV and ultrasound responsive functionalities that can be used as external triggers for controlled release, yet with enhanced mechanical strength that can make them survive in harsh environment. Needle-like TiO_2 nanoparticles (NPs) were produced *in situ* into layer-by-layer (LbL) polyelectrolyte (PE) shells through the hydrolysis of titanium butoxide (TIBO). These rigid TiO_2 NPs yielded the formed capsules with an excellent mechanical strength, showing a free standing structure. A possible mechanism is proposed for their special morphology formation of the TiO_2 NPs and their reinforce effects. Synergistically, their response to UV and ultrasound was visualized via SEM, with results showing an irreversible shell rapture upon exposure to either the UV or ultrasound irradiation. As expected, the release studies revealed that the dextran release from the TiO_2/PE capsules was both UV-dependent and ultrasound-dependent. Besides, biocompatibility of the capsules with the incorporation of amorphous TiO_2 NPs was confirmed by MTT assay experiment. All of these evidences suggested a considerable potential medicine application of the TiO_2/PE capsules for controlled drug delivery.

1 Introduction

Polymer-inorganic composite microcapsules have received extensive attention duo to their widely potential applications in pharmaceutical fabrication processes, controlled drug delivery, agriculture chemicals, and food and cosmetics industries.[1, 2] A versatile approach to produce organized structures with proper control over their stability, size, shell thickness, encapsulation and release properties is the layer-by-layer (LbL) assembly technique.[3, 4] Driven by complementary interactions such as electrostatics, H-bonding and covalent bonding effects, various materials can be assembled alternately onto templates, followed by core removal. Recently, inorganic nanoparticles (NPs) were used as building blocks to functionalize polymeric LbL microcapsules. The introduction of inorganic nanoparticles can not only increase the shell mechanical strength and reduce their permeability, making them suitable for small molecules loading, but would also empower the capsules with new functionalities such as responsiveness to certain stimuli.[5] Various NPs have been incorporated into capsules with enhanced functions in recent years, which includes silica for ultrasound-triggered release, Fe_3O_4 for magnetically navigated drug delivery, and gold for visible and near-infrared (NIR) light responsive capsule systems. [6-8]

Current design and synthesis of inorganic/organic composite capsules has been focused on assembling prefabricated inorganic NPs into soft polyelectrolyte (PE) shells.[9-11] This method can produce capsules with relatively good control over capsule stability and stimuli responsive properties, but poses considerable challenges in controlling the proper distribution of nanoparticles on the shell and achieving the encapsulation and release of low-molecular-weight molecules (including drugs) from LbL capsules.[12] Very recently, we developed a novel technology of *in-situ* production of nanoparticles in PE capsules.[5] Silica nanoparticles were successfully introduced into prefabricated LbL PE microcapsules by *in situ* hydrolysis of tetraethyl orthosilicate (TEOS), producing hybrid capsules with low shell permeability, high mechanical strength and strong ultrasound sensitivity. An example study, the encapsulation of a small molecule cargo (Rh-B) and controlled release through ultrasound treatment showed wide potential applications.

It shall be noted, however, that SiO_2/PE capsules enable ultrasound responsiveness only and no other type of conventional triggers. Designing capsules with multi-functionalities that could be triggered by different stimuli is of high scientific and technical importance.[13,14] Because single

[a] The School of Engineering and Materials Science, Queen Mary, University of London, Mile End Road, London, E1 4NS, Tel: +44 (0)20 7882 5508; Email: g.sukhorukov@qmul.ac.uk
b,Institute of Particle Science and Engineering, University of Leeds, Leeds, LS2 9JT.

Electronic Supplementary Information (ESI) available: [details of any supplementary information available should be included here]. See DOI: 10.1039/x0xx00000x

stimulus-responsive capsules are insufficient for many practical applications as different environmental changes may occur at the same time.[13] For instance, the patients' conditions are usually diverse and complex, thus it is necessary to regulate the drug release rate and dosage according to patients' individual differences.[13] Multifunctional materials can overcome challenges that cannot be solved by their individual components. Therefore, it is much more favourable and promising that microcapsules possess multi-responsive properties simultaneously. [13, 14] If another stimuli sensitivity could be combined with ultrasound-responsive microcapsules, the formed double-stimuli responsive capsules should find a broader range of applications. In many cases, capsules with light sensitivity such as ultraviolet (UV) light are desirable for controlled releases, especially in the fields of surface sciences and environmental applications, where light would be the only available stimulus to trigger the systems.[15,16] The fabrication of such capsules can be generally categorized into two approaches. The first approach is to use polyelectrolytes (PEs) with either photo-responsive or photo-cleavable groups as the layer material.[15] Examples included LbL microcapsules containing azobenzene using poly[1-[4-(3-carboxy-4-hydroxyphenylazo)-benzenesulfonamido]-1,2-ethanediyl, sodium salt] (PAZO) and poly(diallyldimethyl ammonium) chloride (PDADMAC) as the assembling materials, and the UV responsiveness was achieved by UV induced isomerization of PAZO.[16, 17] However, such an approach is constrained by the building materials and PEs where special groups have to be used. The second approach is to assemble inorganic NPs that can absorb UV light. Due to its excellent biocompatibility, great UV-responsive performance, and good ability of immobilizing biomolecules onto their surfaces, TiO_2 nanoparticles have been widely used.[18-20] However only a few reports involved TiO_2-polymer capsules based on pre-fabricated NPs.[2, 21, 22]

Here we propose a novel strategy of incorporating TiO_2 in situ into LbL assembly to prepare multifunctional composite microcapsules that possess both ultrasound and UV responsive functionalities. Without using pre-fabricated TiO_2 NPs, inorganic/PE capsules were made by *in situ* nucleation and growth of TiO_2 inside or on the PE shell surfaces based on the hydrolysis of titanium butoxide (TIBO). Apart from being UV-responsive, it is expected that the incorporation of such *in situ* formed TiO_2 would empower capsules with ultrasound sensitivity, yet with enhanced mechanical strength, increased chemical stability and good biocompatibility. TRITC-Dextran was used as a model cargo to illustrate the encapsulation and dual stimuli induced release from the composite capsules. [23]

2 Experimental Section

2.1 Materials

Poly(4-styrenesulfonate) sodium salt(PSS, Mw = 70K) and poly(allylamine hydrochloride) (PAH, Mw = 58K) were purchased from Sigma-Aldrich. Both polyelectrolytes were used without further purification. $CaCl_2$, sodium carbonate (Na_2CO_3), TRITC-Dextran (Mw=500K), ethylenediaminetetraacetic acid (EDTA), Titanium butoxide (TIBO) and other chemicals were also purchased from Sigma-Aldrich. Nanopure water (Nanopuresystem, Barnstead) with a resistivity of 18.2 $M\Omega cm^{-1}$ was used in all experiments.

2.2 Composite microcapsule preparation

PEs were dissolved in 0.2 M NaCl solution with the concentration of 2 mg/mL. The freshly synthesised $CaCO_3$ cores were first coated with a PAH layer by incubation in 1.5 mL of PAH solution (2 mg/mL) for 15 min, followed by three centrifugation (2000 rpm for 1 min)/wash cycles. Subsequently, they were incubated in 1.5 mL of PSS solution (2 mg/mL) for 15 min, followed by three centrifugation (2000 rpm for 1 min)/wash cycles. The PAH and PSS PE adsorption steps were repeated until the desired number of layers was built on $CaCO_3$ templates. Hollow capsules were finally obtained by dissolving $CaCO_3$ cores in 0.2 M aqueous EDTA, followed by 3 times washing with deionized water and 2 times with ethanol. After that, 1.5 mL of TIBO: ethanol =1:15 solution was added to the PE microcapsules and 24-72 h was allowed for TiO_2 hydrolysis, adsorption, cross linking and condensation process at room temperature (25 ^oC) without any stirring.

For UV stimulated and ultrasound triggered cargo release, TRITC labelled dextran was used as the model cargo. To fabricate dextran encapsulated microcapsules, TRITC-dextran was co-precipitated with $CaCO_3$ microparticles by mixing 0.33 M $CaCl_2$, 0.33 M Na_2CO_3 water solutions and 2 mg/ml TRITC-Dextran water solution while vigorously stirring in 1:1:1 proportion. TRITC-Dextran encapsulated TiO_2/PE microcapsules were made as described above.

2.3 Instrument and Measurement

Ultrasound Triggering. Ultrasonic treatment was performed by an ultrasonic processor GEX 750 (Sonics & Materials, Inc., USA) operating at 20 kHz and 50W. The probe of the ultrasonicator inserts into a capsule suspension in a plastic tube. An ice bath was applied to ensure that the temperature change of the capsule suspensions was less than 5 ^oC.

Zeta-Potential Measurements. Surface potentials of bare and coated $CaCO_3$ microparticles were measured from aqueous solutions on Zetasizer Nano-ZS (Malvern). Each value of the zeta-potential was obtained at ambient conditions by averaging three independent measurements of 100 subruns each.

Scanning Electron Microscopy (SEM) measurement. The morphologies of the capsules were observed by SEM (FEI Inspect-F) using an accelerating voltage of 20 kV. The diluted microcapsule suspension was dropped on a glass slide, air dried, and coated with gold before observation. The capsule size was calculated and determined by using the analysis software Image-Pro Plus Version 6.0 (Media Cybernetics, Inc.). Capsule diameter and distribution were expressed as mean ±SD by randomly averaging the diameters of at least 35 capsules per sample from the SEM data.

Energy dispersive X-ray spectroscopy (EDX). Elemental analysis was performed by means of an EDX Oxford Inca X-act

detector attached to the SEM, operating at an accelerating voltage of 20 kV.

Transmission electron microscopy (TEM). Further morphology and structure of microcapsules as well as the distribution of inorganic particles and shell thickness were studied using a JEOL 2010 transmission electron microscope with LaB_6 filament, operated at 200 kV. For TEM experiments the diluted microcapsule suspension was dropped on a copper grid with holey carbon film and left to dry for 5 minutes.

UV-Visible spectroscopy. An UV-Visible spectrophotometer (LAMBDA950, Perkin-Elmer) was employed to investigate the UV absorption of the composite capsule suspension. Measurements were made by using quartz spectrophotometer cuvettes (Sigma, S10C).

Confocal laser scanning microscopy (CLSM). CLSM images were captured with a Leica TS confocal scanning system (Leica, Germany) equipped with a 63 × /1.4 oil immersion objective.

Measurement of TRITC-Dextran release. To investigate the UV (or ultrasound) stimulated dextran release, the obtained TRITC-Dextran containing capsule suspensions were split into several portions for further study. At specific time intervals, one portion of the capsule samples, with/without UV (or ultrasound) irradiation, was taken out for measurement. The capsule cargo mixture was centrifuged, the supernatant was carefully collected, diluted and then used for TRITC-Dextran quantification. The fluorescence intensity at 572nm of each sample (in supernatant) was determined and normalized with the standard fluorescent solutions with known concentrations. All the samples were kept at the same dilution factors during the experiments and the release amount was determined by the supernatant fluorescence intensity.

3 Results and Discussion

3.1 Composite capsule formation and characterisation

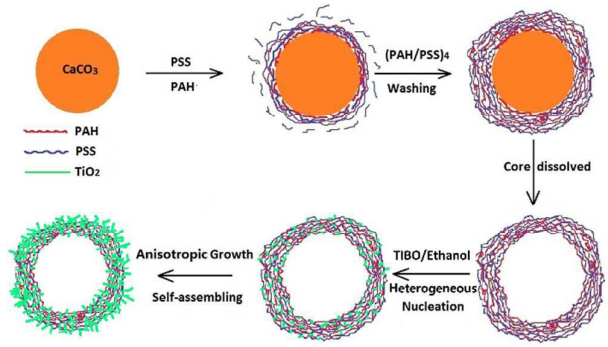

Scheme 1. Schematic representation of the formation process of the TiO_2/polyelectrolyte composite microcapsules.

As shown in scheme 1, both LbL assembly technique and TiO_2 in situ formation were involved in the preparation of composite TiO_2/PE microcapsules. Positively charged PAH and negatively charged PSS were assembled alternately onto the freshly synthesised $CaCO_3$ cores.[5] After reaching a certain layer number, the templates were removed to obtain hollow PE capsules. Then, TiO_2 NPs were incorporated into the polymer shells through the in situ hydrolysis of TIBO under a well-controlled process. Notably, different to most previous reports, no hydrolysis reaction inhibitor or catalyst was used in this reaction system.[24] The typical zata potentials of capsules with different layers (Figure S1, Supporting Information) were monitored to verify the successful deposition of every layer. Obviously, the capsules terminated with PSS showed a negative charge of -25.8mV, which increased to -13.7mV after TiO_2 coating, revealing that TiO2 NPs were fabricated and thusly partially neutralized these capsules' negative charge. Morphology of the formed composite microcapsules was characterized by SEM and TEM.

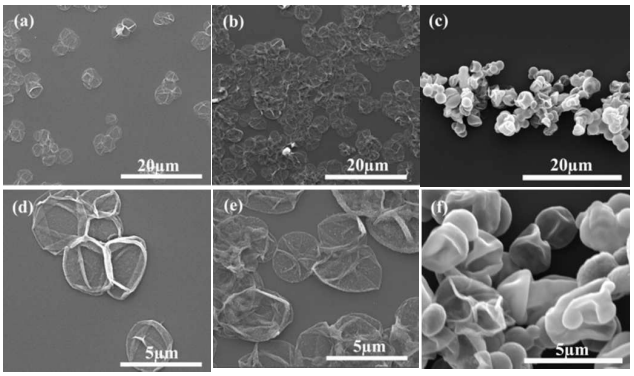

Figure 1. SEM images of capsules: (a,d) without TiO_2; (b,e) with *in-situ* TiO_2 incorporation for 24 hours and (c,f) 72 hours.

The SEM data in Figure 1 demonstrated the significant differences in the size, surface roughness and shape of the capsules without and with TiO_2 coating. Before incorporation with NPs, pure PE capsules showed a diameter of ca. 4.38±0.33μm with relatively smooth shells, which were flattened and in a collapsed form (Figure 1a and d). But in contrast loads of NPs were produced and strongly attached to these polymer shells after incubation them in the TiO_2 precursor solution (TIBO/ethanol) for 24 hours, as shown in Figure 1b and e. These capsules maintained approximately their original shape and size. No free TiO_2 nanoparticles were found along with the composite capsules, which demonstrates that TiO_2 were formed preferably on capsule surfaces. After incubating for 72 hours, a significant shape change was observed, in Figure 1c and f, showing that the formed microcapsules were structurally reinforced into robust free-standing capsules with a confirmed ball-like morphology, smooth surface and reduced particle diameter, i.e, 2.65±0.38 μm. It is plausible that the TiO_2 nanoparticles were formed *in-situ* inside polymer multilayers or on the shell surfaces, which would cross-link and compress the soft polymers, resulting in a decrease in capsule size yet with an increased shell thickness and mechanical strength. Indeed, the increase in shell thickness and the formation of inorganic NPs in PAH/PSS layers was found to enhance the stiffness of the capsules over many orders of magnitude.[25, 26] Dubreuil and coworkers obtained the estimates of the Young's modulus of capsules, showing that it increased from around 100 MPa for

PAH/PSS capsules (collapse upon drying) to 14.5 GPa for PAH/PSS-YF3 capsules (free-standing) if ignored the change in shell thickness. 25 These capsules completely changed the appearance at SEM to be bulky. We believe that the capsules have better integrity while TiO_2 is formed within layer what is reflected on SEM images (Figure 1 (c,f). This evidence indirectly serves for likely enhanced capsules mechanical strength. Compared with our silica/PE composite microcapsules, the external surface of the as-made TiO_2/PE capsule was smoother.[5] This means the formed TiO_2 NPs were finer grained and homogeneously distributed on the polymer shells, arising from a relatively low nucleation and growth rate due to the low supersaturation of the precursor.

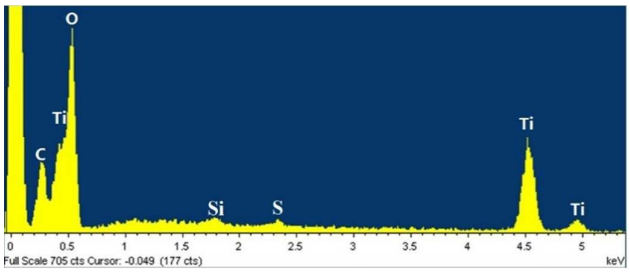

Figure 2. EDX spectrums of the TiO_2/PE composite capsules.

Energy dispersive spectroscopy (EDX) analysis of the composite capsules indicated the presence of large amounts of C, O, and Ti and a tiny amount of S (Figure 2). The results prove that the capsule wall was built up by the polymer layer and TiO_2. The amount of TiO_2 estimated from the TGA data (Figure S2, Supporting Information) is around 50 wt%. No traces of calcium were seen in the spectrum, revealing that $CaCO_3$ was completely removed by EDTA. The small peaks of Si should originate from the glass slide for preparation of SEM sample because no Si source was used for capsule preparation. Furthermore, $(PAH/PSS)_4$ capsules with bigger size (5.53 μm) were produced and examined before and after 72 hours incubation in TIBO/ethanol solution. Their SEM results were highly consistent with the results shown in Figure 1, containing features of spherical morphology, smooth surface, decreased size and increased shell thickness (see Figure S3, Supporting Information). Such result confirmed the repeatability of the procedure of *in situ* TiO_2 incorporation into PE capsules with different sizes.

In order to analyze the morphology, size and distribution of TiO_2 NPs as well as the composite shell thickness, the composite capsules were measured by means of high resolution transmission electron microscopy (TEM), Figure 3. And for comparison the primary PE microcapsules are shown in Figure S4 (Supporting Information). TEM images in Figure 3 revealed that TiO_2 nanoparticles were embedded uniformly in the PE shells and those as-made composite capsules showed an unbroken but hollow structure. High resolution TEM images of Figure 3c and d indicated that the TiO_2 NPs were less than 5 nm in diameter and shaped in an oriented direction, i.e., a needle-like morphology. To our best knowledge, such anisotropic shaped TiO_2 NPs was firstly synthesized at room temperature and synchronously incorporated into PE multilayers. Generally, sol-gel derived precipitates are amorphous in nature and require further annealing treatment to induce crystallization. [27] Here, these needle-like TiO_2 NPs were also of amorphous feature, as demonstrated by the electron diffraction (SAED) pattern, Figure 3e. Comparing Figure S4 with Figure 3a, it is clear that the overall size of the microcapsules decreased and the wall thickness increased upon integrating with TiO_2 NPs, which is consistent with the SEM results, Figure 1. The shell thickness reached to around 70 nm (Figure 3b) which might be many times of the pure PE capsules. Another worth mentioning point is that the needle-like TiO_2 NPs were fully covered the top surface of the dense composite shell (the relative dark part) and formed around 15-25 nm pure TiO_2 layer, as marked in Figure 3d.

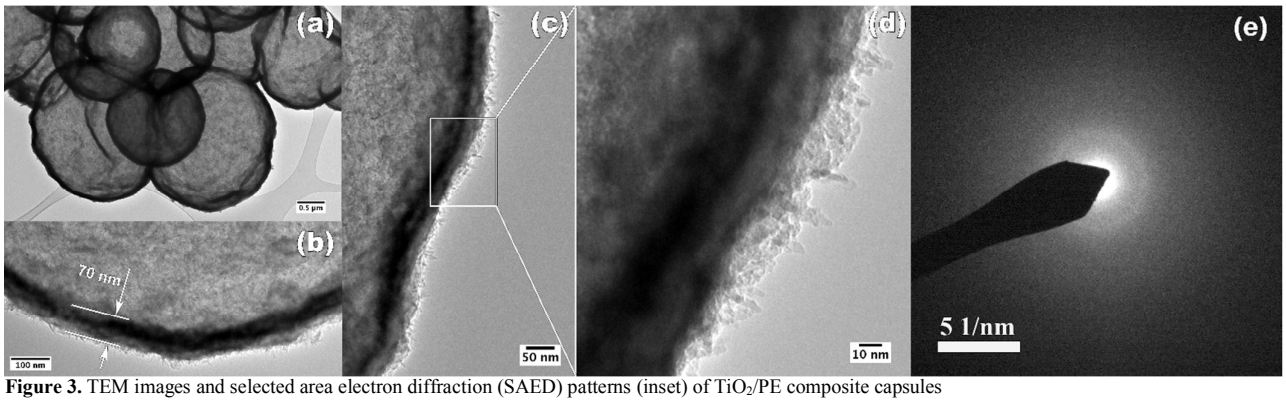

Figure 3. TEM images and selected area electron diffraction (SAED) patterns (inset) of TiO_2/PE composite capsules

3.2 TiO_2 Deposition and Reinforcement Mechanism.

The above SEM, EDX and TEM results confirmed that the composite microcapsules were mainly composed of inorganic TiO_2 NPs and organic PEs. We know that LbL microcapsules can be easily included of prefabricated NPs in a middle layer, but here we show that TiO_2 NPs can directly form and grow within and onto the PE multilayers, which dramatically reinforced their final strength. [6, 8] In addition, these TiO_2 NPs were uniform in size and needle-like in shape. As a matter of fact crystal nucleation and growth anisotropy is

attributed to various factors such as solution composition, concentration of growth species, surfactants and deposition surface conditions. The existence of foreign particles or substrates in the precursor solution may well promote the heterogeneous nucleation on their surfaces. Previously De Guire *et al.* demonstrated that it was possible to have substrate-related oriented growth of anatase TiO_2 toward the hydrophilic substrate surface.[28] So for the production and deposition of these needle-like TiO_2 NPs, it is believed that a deposition took place through heterogeneous nucleation and oriented growth inside or on the soft polyelectrolyte multilayers, rather than through the conventional aggregation of colloidal particles into spherical TiO_2.

A possible nucleation, growth and morphology evolution process of TiO_2 NPs is proposed in Figure 4a. Despite washing PAH/PSS capsules twice with ethanol before incubation them in TIBO/ethanol solution, a small amount of water was still reserved within the PE multilayers as both PSS and PAH are hydrophilic polyelectrolytes. In effect TIBO may immediately react with these H_2O molecules which result in the formation of abundant spherical TiO_2 crystal nucleus within the flexible PE layers as well as their surfaces through heterogeneous nucleation (Figure 4a). It should be pointed out that the soft PAH/PSS multilayers are entangled together which provide many voids such as the concave points on the shell surfaces and the pores inside the PE multilayers.[5] Based on the crystal nucleation and growth principle, a TiO_2 nucleus would initially form at these positions with low energy, for example, the concave points and pores inside the shells.[5, 29] Shin *et al.* suggested the TiO_2 coating formation in his work was based on the agglomeration of the NPs primarily formed by homogeneous nucleation in solution with the aid of large amount of H_2O. [30] However, in our system, homogeneous precipitation of free TiO_2 and their further agglomeration in liquid would not occur due to the minute quantities of H_2O. [31]

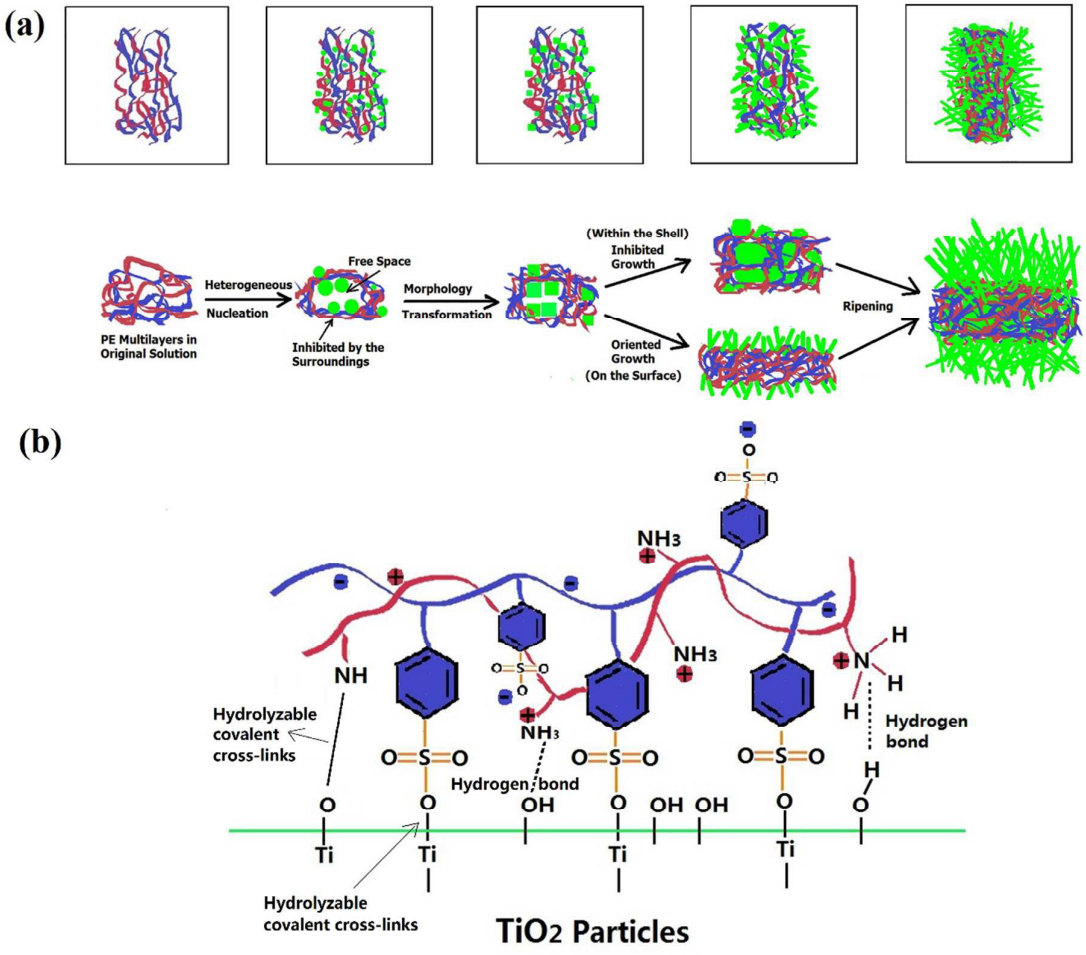

Figure 4. (a) Sketch of the morphology evolution and growth of TiO_2 nanoparticles; (b) Polyelectrolyte structures and the potential interactions with TiO_2 nanoparticles

The slow reaction and precipitation rate result in that the TiO_2 inside the multilayers were tightly integrated with soft polyelectrolytes and that the formation of the external layer composed of the needle-like TiO_2 nanoparticles, which were confirmed by the SEM and TEM data.[31] As shown schematically in Figure 4a, the preliminary formed spherical nucleus will transform into cubic particles, as supported by the thermodynamic theory.[32] Further anisotropic growth of TiO_2

would continue by the selective adsorption of coordinating species on TiO_2 planes, presenting a growth preference in one direction and a growth inhibition in other directions. Practically, inside the PE multilayers, the TiO_2 particle growth direction and their final morphology will be restricted by their surrounding PE building blocks, Figure 4a. Once they grow big enough to occupy the individual free spaces provided by their locations, they will begin to connect with the soft PE building blocks and other adjacent TiO_2 NPs produced inside the layers, then they will compact together and finally form a concrete-like structure. In this process, the PE building blocks act as the scaffold while the *in situ* formed NPs act as the filling materials. Hence, the final shape of the TiO_2 NPs should be depended on the free space they obtained from their locations, which would also be affected by the growth of the adjacent TiO_2 as well as their squeezing action and the consequent transformation of the soft PE layers. Such morphology evolution mechanism is remarkably different from that of the *in situ* formation of NPs on the surfaces of hard porous templates.[33] However, as for the TiO_2 nucleus initially formed on the shell surfaces, with the benefit of more free space, they will act as the tiny crystal seeds, which could sprout individual needle-like TiO_2 particles, as indicated in Figure 4a. With prolonging the reaction time, most of the H_2O was consumed, thusly the hydrolysis rate of Ti precursor reduced greatly. This will promote an oriented particle growth on the surface of the TiO_2 grains by the slow diffusion of Ti cations through the network of TiO_2 grain boundaries.[34] Limited by the total amount of H_2O, no free TiO_2 nanoparticles were found in the system, but the needle-like TiO_2 nanoparticles with an open end were fully covered on the composite shell surfaces, showing in Figure 1 and Figure 3.

In terms of reinforcement effects, with benefit from a large amount of sulfonate groups and amino groups on PE chains, PAH/PSS building blocks act as enhancers and cross linkers to connect adjacent TiO_2 nanoparticles into a stable shell (i.e., through the formation of hydrogen bond, covalent bond etc.), and protects them against movement, see Figure 4b.[18, 35-39] The attractive potential between the sulfonated monolayers and TiO_2 nanoparticles by van der Waals forces, which could be predicted using the Derjaguin, Landau, Verwey, and Overbeek (DLVO) theory, also promoted this interaction process.[30, 31] As a consequence the formed NPs were firmly mixed and combined together with PEs in assist of these potential interaction. Once the capsule pores and surfaces were completely covered by the oriented TiO_2 NPs, further nucleation and growth would continue to occur on the formed composite shell surfaces if both H_2O and TIBO still exist. And the formation and growth mechanism is similar to that occurring inside the PE shells, because the formed composite shells also showed a surface with nanoscale roughness available for further material deposition. Indeed, the TEM date in Figure 3 generally upholds this standpoint, with the formation of 15-25 nm top layer composed of pure TiO_2 (Figure 3d). In addition, the demonstration of enhanced shell density of the composite capsules which was associated with their decreased size and increased shell thickness compared to pure PE capsules is another important observation of this study. Although hydrophobic PE capsules will swell slightly if dispersed them in ethanol, the introduction of TiO2 NPs into PE multilayers would make them twist and curl up together due to the consumption of the residue water from the multilayer pores as the TIBO was hydrolyzed, resulting in a significant shrinkage of the capsules. If prolonging the reaction time, TiO_2 particles would contact and interact with each other with the assistance of PSS and finally cover the whole shell, as illustrated by the TEM results. The continuous inorganic TiO_2 NPs would compress the capsule with a further consequent shrinkage, and thusly the flexible polyelectrolyte layers were restricted. Therefore the pores in capsule shells would become less in amount and smaller in size, and consequently the capsule shell permeability should be drastically reduced. However we need to point out that compared to silica/PE composite capsules a significant difference was the surface roughness.[5] Silica/PE composite capsules displayed a relatively rough surface that was indicated by their SEM images shown in Figure S4 (Supporting Information), because the sol-gel assisted silica coating was associated with a particle attachment mechanism with a high growth rate by material deposition from supersaturated solutions.[31] For the TiO_2 system, after 3 days of reaction, the smooth surface of TiO_2/PE composite capsules (Figure 3c and f) is attributed to the slow growth rate of TiO_2. Such fine-grained and well distributed TiO_2 NPs (72 hours reaction) might afford the as-made composite capsules new superior properties, as will be discussed in the following section.

3.3 Stimuli responsive study

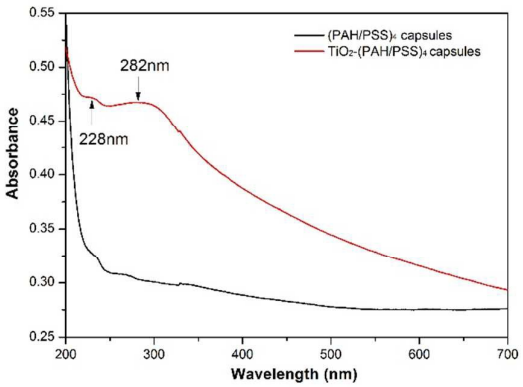

Figure 5. UV-vis spectrum of the TiO_2-$(PAH/PSS)_4$ composite capsules.

TiO_2 has been widely used as a UV-absorbing agent for environmental applications and here they were used to absorb UV light to increase the permeability of polymer capsules.[40, 41] The UV absorbance spectra of the composite capsules were measured by means of UV/Vis spectroscopy, as given in Figure 5. The TiO_2/PE composite capsules showed two absorbance peaks with a wide tailing area up to 700nm whereas no obvious absorbance peak was

Nanoscale

PAPER

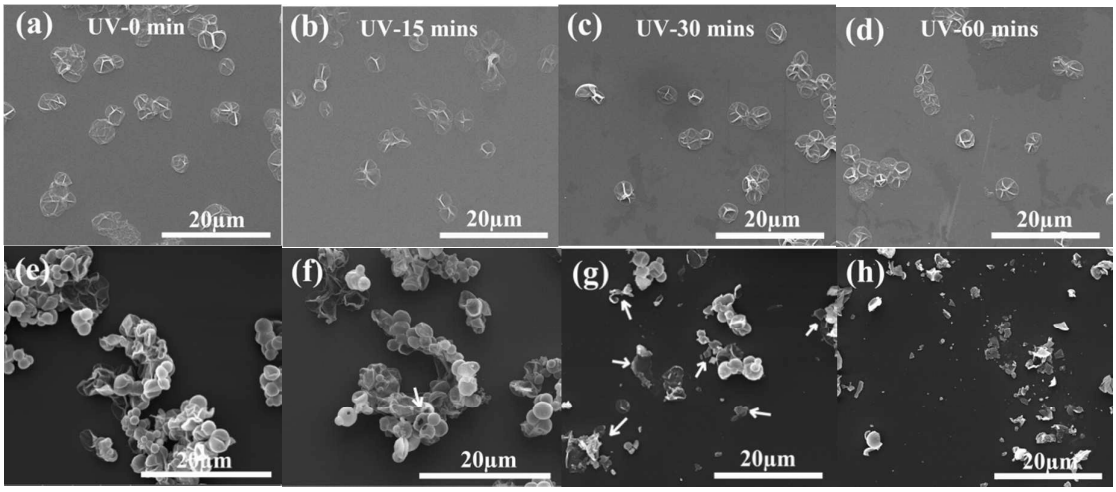

Figure 6. SEM images of capsules irradiated with UV light for different times: (a, b,c,d) (PAH/PSS)4 capsules treated for 0min, 15 min, 30min and 60 min respectively; (e,f,g,h) TiO_2-(PAH/PSS) composite capsules treated for 0min, 15 min, 30min and 60 min respectively. The arrows represent broken capsules.

found for PAH/PSS capsules without TiO_2 incorporation. Further upheld by UV absorbance data of TiO_2/PSS observed by Wang *et al*, we can conclude that the peaks at 228 nm and 282nm can be mainly attributed to the incorporated TiO_2 nanoparticles.[42] Thus, the formed composite capsules were imparted with a strong UV absorbance property. The effect of UV irradiation on the morphology of these capsules was examined by means of SEM.

Figure 6 shows SEM images of the capsules with and without TiO_2 NPs after exposure to UV light (320-400nm, ~110 mW cm^{-2}) for different times (i.e., 0min, 15min, 30min and 60min). It is clearly seen that the capsules without TiO_2 were unaffected by UV irradiation, as evident from the little morphology changes before and after UV treatment. However, a significant difference was found for the TiO_2/PE composite capsules. For those, capsules had spherical shapes prior to the UV irradiation, and more than half of them were decomposed after UV irradiation for 30 minutes and nearly all of them were broken into small fragments when the time reached to 60 minutes (Figure 6h). Comparing the different reactions between these two kinds of capsules responding to UV irradiation, it can be safely drawn concluded that the incorporation of TiO_2 made PE capsules with photocatalytical activeness. Upon UV radiation, electron-hole pairs in TiO_2 were generated and the holes residing in the valence band of TiO_2 performed high oxidative activity.[43] It is believed that the deconstruction of composite capsules can be caused by two reasons. One is that the PEs might be partly decomposed by the photocatalytic effect of TiO_2 in the composite layer. The other is the large amount of electron-hole pairs in TiO_2 stimulated by UV light may transfer to the PEs, which prompts the disconnection of PEs and inorganic NPs. For example, the bonding forces like hydrogen bonds and van der Waals forces between TiO_2 and PEs would decrease. Promisingly, such a capsule system could find applications in the fields of cosmetics and agriculture, where naturally-present UV light can trigger the release of encapsulated materials.

Previously we have demonstrated that the ultrasound sensitivity of the PSS/PAH capsules can be remarkably increased if rigid SiO_2 nanoparticles were embedded in the PE network.[5] In this study we again prove that the composite capsules with *in situ* formed TiO_2 NPs also show strong ultrasound sensitivity. The suspensions of microcapsules without and with TiO_2 composition were treated by means of ultrasound sonication for different duration times (3, 6, and 10s). The resulting SEM data are shown in Figure 7. Pure $(PAH/PSS)_4$ capsules were not affected if the sonication time was less than 6 seconds (Figure 7b and c) and only slight deformations were observed after 10 seconds of sonication (Figure 7d). However for the TiO_2/PE composite capsules, obvious breakage was observed at t = 3 seconds, and complete destruction was achieved at t = 10 s. The increased ultrasonic sensitivity of the TiO_2/PE microcapsules is clear. The strong response to ultrasound might be attributed to the increased density gradient across the water/shell interface, the enhanced of the shell stiffness, and the decreased shell elasticity, all of which would improve the absorption of acoustic energy, leading to the increased ultrasound responsiveness.[5,11,44-47]

Nanoscale

PAPER

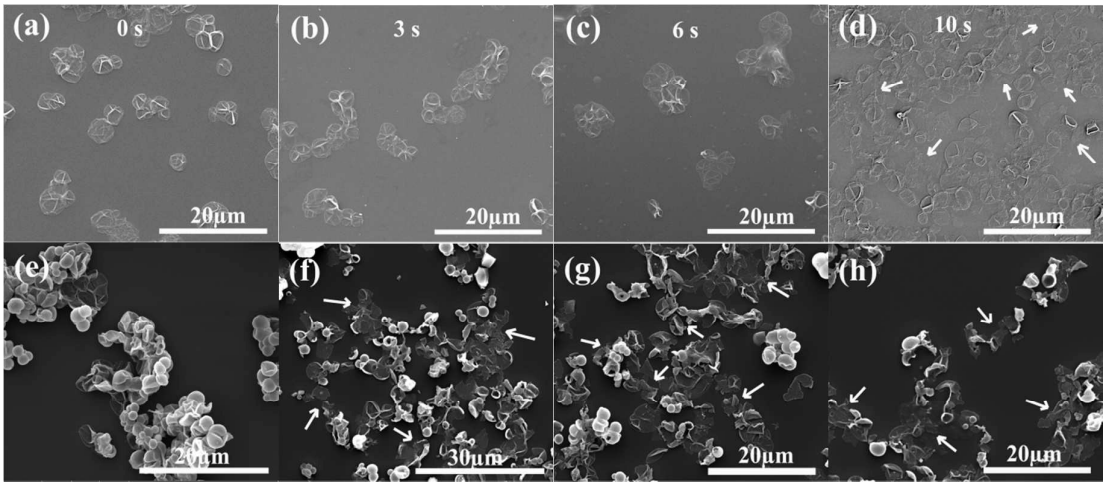

Figure 7. SEM images of capsules treated by ultrasound for different times: (a, b,c,d) $(PAH/PSS)_4$ capsules treated for 0s, 3s, 6s and 10s respectively; (e,f,g,h) TiO_2-$(PAH/PSS)_4$ composite capsules treated for 0s, 3s, 6s and 10s respectively. The arrows show broken capsules.

Despite of these two types of stimuli response, TiO_2/PAH/PSS hybrid capsules also displayed a different response to the pH of the environment compared to the pure PAH/PSS capsules. We know from other work that LbL microcapsules composed of weak PEs are generally sensitive to the pH of the environment.[15, 48, 49] For the PSS/PAH capsule system, when the pH of the environment becomes higher than the pKa of polybases, i.e. PAH, the PEs become uncharged thus resulting in the disassembly of the capsules. However, as shown in Figure S6 (Supporting Information), the strengthened hybrid capsules (*in situ* TiO_2 incorporation for 72 hours) kept their initial shape after treated by strong alkali solution (NaOH, pH =13) for 10 minutes, whereas the pure PAH/PSS capsules were totally destroyed into floccules after only 2 minutes of treatment, consistent with the pH-responsive study of PSS/PAH capsules by De´jugnat et al..[49] Interestingly, hybrid capsules obtained after 24 hours *in situ* TiO_2 incorporation were similarly dissolved into small floccules after 10 minutes of soaking in the NaOH solution. This might be due to the small amount of TiO_2 deposited on PE multilayers, which was not continuously covered the shell and was not strong enough to rigidly support the shell in harsh acidic or alkaline environments, leading to their separation of the PE building blocks. Experiment data showed that the capability of pH resistance of the composite capsule increased with the increase of TiO_2 concentration, indicating a promising potential of applying their tunability by either ultrasound or UV stimulus in harsh conditions.

To study the feasibility of loading cargos in TiO_2/PE capsules, TRITC-dextran (500kDa) was selected as an example cargo due to its mature application in LbL capsule systems. Their encapsulation was carried out through a co-precipitation process. The corresponding CLSM images of capsules loaded with TRITC-Dextran are given in Figure 8. Before dissolving the $CaCO_3$ cores by EDTA, the bright red balls and strong fluorescent signals (Figure 8a and the inset) were observed. Figure 8b revealed most of the TRITC-dextran molecules were still entrapped inside the cavities that after removing the cores despite of a slight loss during the process of core dissolving. The inset shows an average fluorescent signal intensity of 86 units inside the capsule. It is worth mentioning that the permeability of PAH/PSS capsules would increase if they were transferred into ethanol, which means the cargos inside their cavities would leak out. [50] But TRITC-dextran is not soluble in ethanol, hence most still stays inside the cavities during the formation process of TiO_2. After the *in-situ* synthesis and incorporation of TiO_2, the freshly synthesized composite capsules with TRITC-dextran loading contained ~140 units of fluorescent intensity, as shown in Figure 8c. A possible reason for the increased fluorescent intensity is the increased concentration of TRITC-dextran due to the decrease in capsule size. The composite capsules were also measured after 50 days' storage in the dark. Some TRITC-Dextran molecules leaked out and an average fluorescent signal intensity of ~ 80 units was kept inside.

3.4 Encapsulation and release study

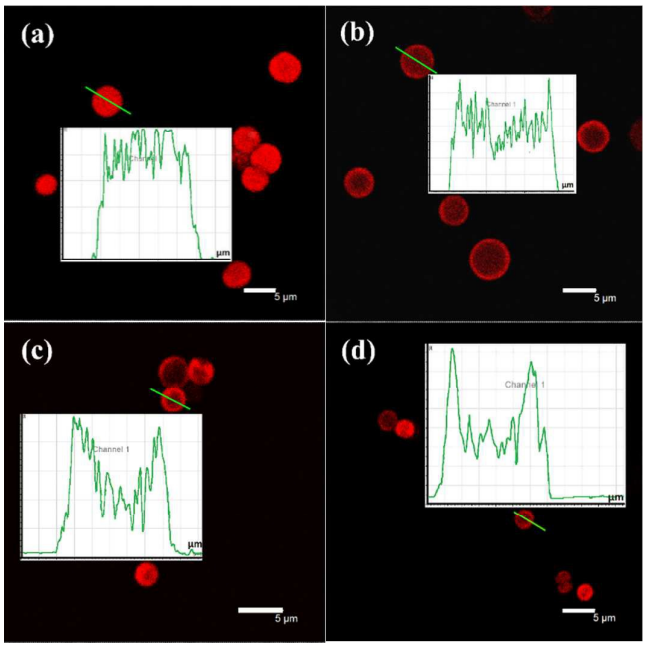

Figure 8. CLSM images of capsules loaded with TRITC-Dextran. (a) $(PAH/PSS)_4$ before removing the $CaCO_3$ cores; (b) $(PAH/PSS)_4$ after removing the cores; (c) TiO_2-$(PAH/PSS)_4$ capsules; and (d) TiO_2-$(PAH/PSS)_4$ capsules after being kept for 50 days in the dark. The insets showed relative fluorescent intensity recorded by line scan of the corresponding capsules.

As already been demonstrated above, the incorporated TiO_2 NPs in the capsule shells enabled them be responsive to UV light and ultrasound, which could offer a promising strategy for the controlled release of the encapsulated substances, especially for the applications where the abundant UV light (e.g., sunlight) or ultrasonic could be used. To determine the possibility, UV and ultrasound stimulated dextran release was studied. The initial amount of encapsulated TRITC dextran in PAH/PSS capsule cavities was calculated as 4.47 mg in total with an encapsulation efficiency of ~56%. The TRITC-Dextran containing PAH/PSS capsule suspension was divided into two parts: one was for the release study of pure PE capsules and the other was coated with TiO_2 nanoparticles for their further release study of PE/TiO_2 composite capsules. Then the PE and TiO_2/PE capsule suspensions were diluted into 30 mL, respectively, both of which referred to the working samples. Then 0.5 mL of the working sample was collected after UV or ultrasound treatment at every sampling time point. Indeed, if there was no TRITC-Dextran loss from the pure PE capsules, each portion used for TRITC-Dextran quantification should contain 37.250 μg of dextran in the capsules. For composite capsules, it is worth mentioning that a small amount of TRITC-Dextran would diffuse out of the capsules during the TiO_2 coating process even through dextran is not soluble in ethanol, with an estimated loss of ~5 %. So each portion of composite capsules used for TRITC-Dextran quantification contains 35.387 μg of dextran. In order to facilitate the comparison between pure and composite capsules, the release amount (M_R) was plot as a percentage of the initial encapsulation amount (M_I), as shown in Figure 9.

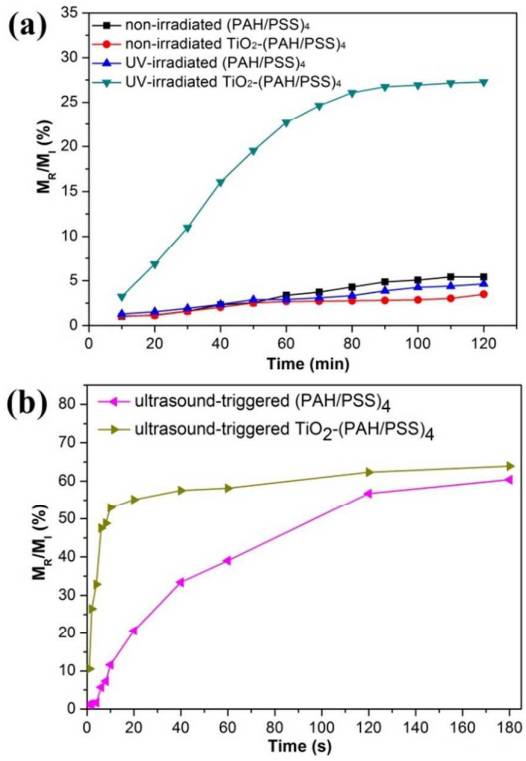

Figure 9. Trigger-induced TRITC-Dextran release as a function of irradiation time.

TRITC-dextran molecules were not tightly sealed in these capsule cavities, so partial release induced by diffusion through the porous multilayer shells was inevitable. A slow release rate of TRITC-Dextran was observed for all non-irradiated samples. Notably, compared to pure PE capsules, the incorporation of TiO_2 reduced the leaking amount which is more likely due to the reduction of shell permeability and the increase of shell thickness. As for the UV-irradiated samples, the release from pure PE capsules was nearly identical with the non-irradiated samples because they were not responsive to UV light, showing a released amount about 4.6% after 2 hours of UV irradiation. In contrast, the UV accelerated the dextran release from TiO_2/PE capsules rapidly, reaching a plateau after ~100 minutes irradiation. It is clearly seen that only 27.3% of the initial dextran was released outside even though nearly all composite capsules were broken when treatment time reached to 60 minutes (Figure 6h). Such a small percentage was caused by both the photobleaching effect due to long-time UV irradiation, and the attachment of dextran to the amino-terminated inner surface of the microcapsules. Actually such possible attachment could be facilitated by both hydrogen bonds and the hydrolyzable covalent cross-links resulting from aldehydes and primary amines coupling.[38]

Compared to UV-irradiated samples, the released TRITC-Dextran amount of both the ultrasound-treated samples increased quickly during the duration time. But the capsules with TiO_2 coating displayed a much faster release rate when compared to the PE capsules (more than 10 fold within the first 10 seconds) as a result of

their higher sensitivity to ultrasound. Around 26% of the fluorescent dextran was released in just 2 seconds, and it increased to 48% in 6 seconds. The release curve became flatted after 10 seconds when reaching a value of ~53%. However, for the pure PE capsules, the encapsulated TRTTC-Dextran was released slowly in the initial 10 seconds. Only ~1% was detected after 2 seconds, and 6% in 6 seconds. After reaching 11% at t= 10s, the release rate increased because the PE capsules start ton be broken by the ultrasonic processing (Figure 7). Total release amounts of ~60% were observed for both capsules after 180 seconds of sonication due to the full breakage of both capsules (Figure S7, Supporting Information). All the $(PAH/PSS)_4$ capsules were broken into small pieces when the sonication time reach to 120 seconds, while all the composite capsules can be destroyed in 60 seconds. But particularly worth mentioning is that the composite capsules showed an efficient release within a short duration of applied ultrasound, which might be desirable for certain medical applications (minimizing the damage to healthy tissues).

All of these results revealed a good responsive property of the formed composite capsules. In practical applications, one of the stimuli (UV or ultrasound) could be used as a main method to release the encapsulated cargos, while the other one could be used as an assist or be ignored. More interestingly and importantly, in some special cases, both of UV and ultrasound could be used simultaneously to enhance the release rate and dosage of drugs. In addition, we also demonstrated the composite capsules with modification of TiO_2 NPs were well tolerated by B50 cells at a capsule : cell ratio of 10 : 1 and no obvious signs of toxicity were displayed (data given in Figure S8, Supporting Information). If we raise the capsule : cell ratio to 50:1, the PE capsules showed a significant toxicity to cells especially in the firat 24 hours, however the TiO_2/PE capsules performed a much better cell viability than the PE capsules. Such results revealed that TiO_2 NPs are not toxic and with TiO_2 coating can improve the biocompatibility. TiO_2/PE capsules could be further surface-modified to ensure complementary binding to ligands and make them be suitable for targeted delivery of chemicals and controlled release.[18] It is believed that the idea proposed in this work, i.e. novel TiO_2/PE composite capsules with good biocompatibility and the capability of UV and ultrasound triggered release, could be extended to cosmetics, agriculture, environment and various medical applications.

4 Conclusions

In this study we proposed and validated a novel approach for fabricating multi-functional inorganic-polymer composite capsules via in situ production of NPs in PE shells. Needle-like TiO_2 NPs. were synthesised into prefabricated PAH/PSS microcapsules through the in situ hydrolysis of TIBO, which made the obtained microcapsules become of enhanced mechanical strength and demonstrate UV and ultrasound responsiveness as well as good biocompatibility. The formation of needle-like nanoparticles was through a deposition mechanism via a heterogeneous nucleation approach rather than forming agglomeration from a bulk solution. Similar to the result of PE/silica composite capsules, the incorporation of TiO_2 nanoparticles filled gaps inside the polymer multilayers during the hydrolysis and precipitation process, which might yield denser shells with reduced permeability.[5] The formed TiO_2/PE capsules showed a free-standing structure with smaller size, smoother surface and larger shell thickness. Besides the needle-like TiO_2 also acted as UV absorbing agent and ultrasound sensitivity enhancer, yielding the composite capsules multifunction. Exposure of the formed TiO_2/PE capsules to either UV or ultrasound triggering showed an irreversible shell rapture and efficient cargo release. Such multifunctional capsules are promising for various future applications including drug delivery systems, cosmetic products and environment engineering.

Acknowledgements

H.G. thanks financial support from China Scholarship Council for her Ph.D. study.

References

1 S. She, Q. Li, B. Shan, W. Tong and C. Gao, Adv. Mater., 2013, 25, 5814-5818.
2 A. M. Pavlov, S.A. Gabriel, G.B. Sukhorukov and D.J. Gould, Nanoscale, 2015, 7, 9686-9693.
3 A. L. Becker, A. P. R. Johnston and F. Caruso, *Small*, 2010, 6, 1836.
4 E. Donath, G. B. Sukhorukov, F. Caruso, S.A. Davis and H. Möhwald, *Angew. Chemi. Int. Ed.*, 1998, *37*, 2202-2205.
5 H. Gao, D. Wen and G. B. Sukhorukov, *J. Mater. Chem. B*, 2015, *3*, 1888-1897.
6 A. M. Pavlov, V. Saez, A. Cobley, J. Graves, G. B. Sukhorukov and T. J. Mason, *Soft Matter*, 2011, *7*, 4341-4347.
7 D. A. Gorin, S. A. Portnov, O. A. Inozemtseva, Z. Luklinska, A. M.Yashchenok, A. M. Pavlov, A. G. Skirtach, H. Mohwald and G. B. Sukhorukov, *Phys. Chem. Chem. Phys.*, 2008, *10*, 6899-6905.
8 A. S. Angelatos, B. Radt and F. Caruso, *J. Phys. Chem.*, *B* 2005, *109*, 3071-3076.
9 M. N. Antipina and G. B. Sukhorukov, *Adv.Drug Deliv. Rev.*, 2011, *63*, 716-729.
10 K. Zhang, W. Wu, K. Guo, J. Chen and P. Zhang, *Langmuir*, 2010, *26*, 7971-7980.
11 T. A. Kolesnikova, D. A. Gorin, P. Fernandes, S. Kessel, G. B. Khomutov, A. Fery, D. G. Shchukin and H. Möhwald, *Adv. Funct. Mater.*, 2010, *20*, 1189-1195.
12 P. R. Gil, L. L. del Mercato, P. del Pino, A. Muñoz Javier and W. J. Parak, *Nano Today*, 2008, 3, 12-21.
13 J. Wei, X. Ju, X. Zou, R. Xie, W. Wang, Y. Liu, and L. Chu, *Adv. Funct. Mater.* 2014, *24*, 3312-3323.
14 Y. Yeh, R. Tang, R. Mout, Y. Jeong, and V. M. Rotello, *Angew. Chem. Int. Ed.*, 2014, *53*, 5137-5141.
15 W. N. Xu, I. Choi, F. A. Plamper, C. V. Synatschke, A. H. E. Müller and V. V. Tsukruk, *ACS NANO*, 2013, *7*, 598-613.
16 Q. Yi and G. B. Sukhorukov, *Soft Matter*, 2014, *10*, 1384-1391.
17 Q. Yi and G. B. Sukhorukov, *ACS NANO*, 2013, *7,* 8693-8705.
18 L. Ye, R. Pelton and M. A. Brook, *Langmuir*, 2007, *23*, 5630-5637.
19 Y. X. Hu, J. P. Ge, Y. G. Sun, T. R. Zhang and Y. D. Yin, *NanoLett.*, 2007, *7*,1832-1836.
20 V. Klimkevicius, T. Graule and R. Makuska, *Langmuir*, 2015, *31*, 2074-2083.
21 T. Chen, P. J. Colver and S. A. F. Bon, *Adv. Mater.*, 2007, *19*, 2286-2289.
22 D. G. Shchukin, E. Ustinovich, D. V. Sviridov, Y. M. Lvov and G. B. Sukhorukov, *Photochem. Photobiol. Sci.*, 2003, *2*, 975-978.
23 J. J. Yuan, S. X. Zhou, L. M. Wu and B. You, *J. Phys. Chem.*, *B2* 2006, *110*, 388-394.
24 J. G. Yu, J. C. Yu, M. K.P. Leung, W. K. Hob, B. Chenga, X. J. Zhao and J. C. Zhao, *J. Catal.*, 2003, *217*, 69-78.
25 F. Dubreuil, D. G. Shchukin, G. B. Sukhorukov and A. Fery, *Macromol. Rapid Commun.*, 2004, *25*, 1078-1081.

26 G. B. Sukhorukov, A. Fery, M. Brumenb and H. Möhwald, *Phys. Chem. Chem. Phys.*, 2004, *6*, 4078-4089.
27 H. M. Liu, W. S.Yang, Y. Ma, Y. A. Cao, J. J. Yao, J. Zhang and T. D. Hu, *Langmuir*, 2003, *19*, 3001-3005.
28 H. Pizem and C. N. Sukenik, *Chem. Mater.*, 2002, *14*, 2476-2485.
29 X. Wang, W. Zhou, J. Cao, W. Liu and S. Zhu, *J. Colloid Interface Sci.*, 2012, *372*, 24-31.
30 I. Larson, C. J. Drummond, D. Y. C. Chan and F. Grieser, *J. Am. Chem. Soc.*, 1993, *115*, 11885-11890.
31 H. Strohm and P. Löbmann, *Chem. Mater.*, 2005, *17*, 6772-6780.
32 Y. G. Sun and Y. N. Xia, *Sci.*, 2002, *298*, 2176-2179.
33 S. Chang, Z. A. Combs, M. K. Gupta, R. Davis, and V. V. Tsukruk, *ACS Appl. Mater. Interfaces*, 2010, *11*, 3333-3339.
34 D. Guan and Y. Wang, *Nanoscale*, 2012, *4*, 2968-2977.
35 J. J. D. Yoreo, and P. G. Vekilov, *Rev. Mineral. Geochem.*, 2003, *3*, 57-93.
36 G. Mattioli, F. Filippone, R. Caminiti and A. A. Bonapasta, *J. Phys. Chem.*, *C* 2008, *112*, 13579-13586.
37 S. Spange and S. Grund, *Adv. Mater.*, 2009, *21*, 2111-2116.
38 D. Usov and G. B. Sukhorukov, *Langmuir*, 2010, *26*, 12575-12584.
39 T. Levy, C. Déjugnat and G. B. Sukhorukov, *Adv. Funct. Mater.*, 2008, *18*, 1586-1594.
40 K. C. Krogman, N. S. Zacharia, D. M. Grillo and P. T. Hammond, *Chem. Mater.*, 2008, *20*, 1924-1930.
41 D. N. Priya, J. M. Modak and A. M. Raichur, *ACS Appl. Mater. Interfaces*, 2009, *1*, 2684-2693.
42 Z. S. Wang, T. Sasaki, M. Muramatsu, Y. Ebina, T. Tanaka, L. Zhou and M. Watanabe, *Chem. Mater.*, 2003, *15*, 807-812.
43 K. Katagiri, K. Koumoto, S. Iseya, M. Sakai, A. Matsuda and F. Caruso, *Chem. Mater.*, 2009, *21,* 195-197.
44 M. F. Bédard, A. Munoz-Javier, R. Mueller, P. del Pino, A. Fery, W. J. Parak, A. G. Skirtach and G. B. Sukhorukov, *Soft Matter*, 2009, *5*, 148-155.
45 D. G. Shchukin, D. A. Gorin and H. Möhwald, *Langmuir*, 2006, *22*, 7400-7404.
46 B. G. de Geest, A. G. Skirtach, A. A. Mamedov, A. A. Antipov, N. A. Kotov, S. C. de Smedt and G. B. Sukhorukov, *Small*, 2007, *3*, 804- 808.
47 A. G. Skirtach, B.G. De Geest, A. Mamedov, A. A. Antipov, N. A. Kotov and G. B. Sukhorukov, *J. Mater. Chem.*, 2007, *17*, 1050-1054.
48 M. A. Pechenkin, H. Möhwald and D. V. Volodkin, *Soft Matter*, 2012, *8*, 8659-8665.
49 Déjugnat and G. B. Sukhorukov, *Langmuir*, 2004, *20*, 7265-7269.
50 A. A. Antipov and G. B. Sukhorukov, *Adv. Colloid Interface Sci.*, 2004, *111*, 49-61.